

Robust Optimal Offering and Operation Framework for Hybrid Power Plants in Voluntary Balancing Markets with Decision Dependent Uncertainties

Rujie Zhu ¹, Kaushik Das ², Oskar Lindberg ², Poul Ejnar Sørensen ², and Anca Daniela Hansen ²

¹DTU Wind

²Affiliation not available

October 31, 2023

Abstract

In recent years, utility-scale hybrid power plants (HPPs) have emerged as promising electricity generation resources by combining multiple generation technologies and storage capabilities. This paper presents a novel framework for optimizing the offering and operation of HPPs in the voluntary balancing market, specifically for providing regulating power as a balancing service. The proposed framework utilizes a two-level robust optimization approach, where the first level focuses on look-ahead offering and operation, and the second level handles real-time re-scheduling of generation. Uncertainties arising from wind power and regulating prices are considered as decision-independent uncertainties (DIU). Conversely, the decisions regarding regulating power offers influence the uncertainty associated with activated regulating volumes, leading to decision-dependent uncertainties (DDU). To tackle the model incorporating both DIU and DDU, this paper introduces a customized nested adaptive column and constraint generation (NAC&CG) algorithm that ensures global convergence. The case studies demonstrate the effectiveness of the proposed model in enabling HPPs to accurately track the activated regulating volumes, ensuring reliable provision of balancing service.

Robust Optimal Offering and Operation Framework for Hybrid Power Plants in Voluntary Balancing Markets with Decision Dependent Uncertainties

Rujie Zhu, *Student member, IEEE* Kaushik Das, *Senior member, IEEE* Oskar Lindberg, *Student member, IEEE* Poul Ejnar Sørensen, *Fellow, IEEE* and Anca Daniela Hansen

Abstract—In recent years, utility-scale hybrid power plants (HPPs) have emerged as promising electricity generation resources by combining multiple generation technologies and storage capabilities. This paper presents a novel framework for optimizing the offering and operation of HPPs in the voluntary balancing market, specifically for providing regulating power as a balancing service. The proposed framework utilizes a two-level robust optimization approach, where the first level focuses on look-ahead offering and operation, and the second level handles real-time re-scheduling of generation. Uncertainties arising from wind power and regulating prices are considered as decision-independent uncertainties (DIU). Conversely, the decisions regarding regulating power offers influence the uncertainty associated with activated regulating volumes, leading to decision-dependent uncertainties (DDU). To tackle the model incorporating both DIU and DDU, this paper introduces a customized nested adaptive column and constraint generation (NAC&CG) algorithm that ensures global convergence. The case studies demonstrate the effectiveness of the proposed model in enabling HPPs to accurately track the activated regulating volumes, ensuring reliable provision of balancing service.

Index Terms—hybrid power plant, balancing service, decision dependent uncertainty, robust optimization.

NOMENCLATURE

A. Parameters and Constants

$\beta_{t,s}^{up}$	Upward balancing price at period t in scenario s .
$\beta_{t,s}^{dw}$	Downward balancing price at period t in scenario s .
π_t^{sp}	Spot price at period t .
$\pi_{t,s}^{rp}$	Regulating price at period t in scenario s .
q_s	Probability of scenario s .
\hat{P}_t^w	Wind power forecasts at period t .
η_l	Battery leakage efficiency.
η_{cha}	Battery charging efficiency.
η_{dis}	Battery discharging efficiency.
E_t^{min}	Minimum remaining energy of battery.
E_t^{max}	Maximum remaining energy of battery.
$P^{b,max}$	Power capacity of battery.
$P^{w,max}$	Power capacity of wind.
$P^{up,max}$	Maximum up regulating power offer.
$P^{dw,max}$	Maximum down regulating power offer.
$P^{up,min}$	Minimum up regulating power offer.
$P^{dw,min}$	Minimum down regulating power offer.
P_{grid}	Grid connection capacity.

B. Variables

P_t^{ha}	power schedule of HPP at period t .
------------	---------------------------------------

P_t^w	wind power schedule at period t .
P_t^{cha}/P_t^{dis}	Battery charging/discharging schedule at period t .
z_t	Battery charging/discharging state .
E_t^b	Energy of battery at period t .
P_t^{up}	Up regulating power offer at period t .
P_t^{dw}	Down regulating power offer at period t .
$P_t^{w,up}$	Up regulating power offer from wind at period t .
$P_t^{w,dw}$	Down regulating power offer from wind at period t .
$P_t^{b,up}$	Up regulating power offer from battery at period t .
$P_t^{b,dw}$	Down regulating power offer from battery at period t .

I. INTRODUCTION

RENEWABLE energy sources (RESs) and energy storage systems (ESSs) play significant roles in the green transition of energy systems. Generally, they are placed at different locations due to developers' interests and power grid requirements. In recent years, there are commercial interests in combining RES and ESS on the plant level, forming hybrid power plants (HPPs) [1]. Although there is temporarily no consensus on the definition of HPPs, HPPs are generally co-located two or more generation and storage technologies that produce electricity in coordinated ways. Different from virtual power plants (VPP) which are cloud-based distributed power plants aggregating distributed energy resources [2], HPPs are co-located utility-scale power plants. Due to the high cost of point of interconnection, HPPs are normally overplanted in respect to grid connection capacity, which is also an obvious distinction with VPP. It is clear that HPPs can produce more reliable and flexible power compared with individual renewable power plants. Besides, according to the report from National Renewable Energy Laboratory [3], HPPs can accelerate the integration of renewable energy into energy systems. Currently, the trading of electricity produced by HPPs is mainly based on power purchase agreements [4]. However, the increasing advocacy for the active involvement of HPPs in electricity markets to provide balancing services is becoming more pronounced.

As demonstrated in Fig. 1, to provide balancing service in European electricity markets, market participants can offer balancing capacity in the day-ahead (DA) reserve market (RM) before 9:30 a.m. on the previous day. Then the participants can enter balancing markets (BMs) with regulating power offers no less than the committed balancing capacity. However, market

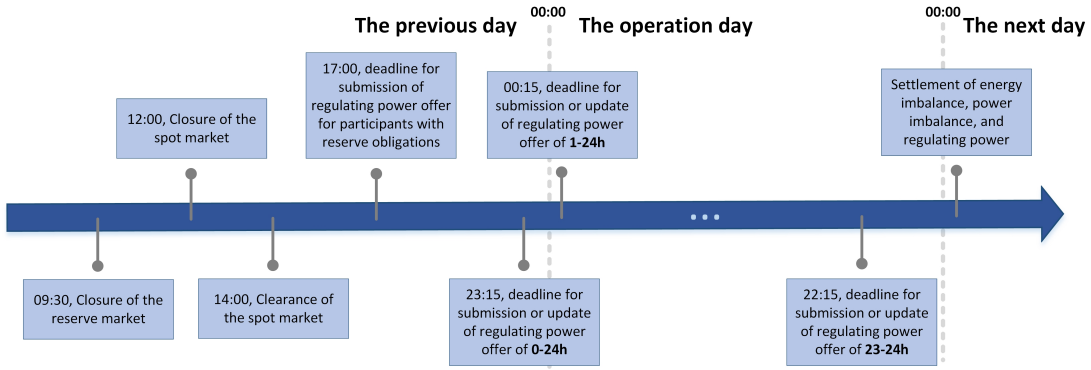


Fig. 1. Schematic of important deadlines for participants offering in voluntary balancing markets (Denmark example)

participants can refrain from committing balancing capacity in DA RM, instead entering balancing markets voluntarily when they find it is profitable [5]. For example in Denmark, irrespective of whether participants have a reserve obligation or not, the offer of regulating power can be updated until 45 minutes prior to the delivery hour [6]. Since the regulating power is used by the transmission system operator (TSO) to ensure system security, there are non-financial requirements for participants to deliver the activated regulating power. In case participants cannot provide the service or provide non-conforming service, the TSO may rule out the participants from taking part in the auctions [7]. Therefore, to avoid this situation, the reliability of the regulating power offer is crucial.

Table I provides a comprehensive overview of the existing research studies focusing on the optimal offering and operation of HPPs in electricity markets. Notably, all the reviewed studies consider the spot market (SM) since the energy sold in SM is the reference energy during the operation. Furthermore, some investigations delve into the intra-day market (IDM), providing opportunities to modify the reference energy. To address uncertainties associated with renewable power and market prices, robust optimization [13], [16] and stochastic optimization [13]- [18] techniques are commonly employed. Additionally, the provision of ancillary services is also considered in certain studies. Ref. [21] studies HPPs' optimal operation in the RM and SM using stochastic optimization. The uncertainty of regulating volumes is represented by a set of scenarios using k-means clustering. Similar methodologies are also applied in ref. [22] to further consider IDM. It is important to note that the final revenues of HPPs also encompass the imbalance settlement (IS), a key component of BMs. Consequently, a majority of the literature accounts for the IS within their proposed models.

The literature review reveals a notable research gap concerning the optimal offering and operation of hybrid power plants (HPPs) in BMs. Notably, ref. [24] focuses on a deterministic model that overlooks uncertainties. Furthermore, another referenced model in [23] lacks a guarantee of reliable regulating power offers, potentially exposing HPPs to the risk of being quarantined by the TSO during real-world operations. While [18] claims to include BMs, the methodology primarily focuses on IS within BMs rather than the optimal offering strategy. Therefore, this paper uses "voluntary balancing market (VBM)" to distinguish it from IS. In the study of offering strategy in VBMs, it is important to highlight that none of the literature considers the uncertainty associated with activated regulating volumes, which differentiates it from uncertainties related to wind power and regulating prices. Wind power and

regulating prices fall under decision-independent uncertainty (DIU), whereas the uncertainty of activated regulating volumes falls under decision-dependent uncertainty (DDU). This disparity implies that the uncertainty of activated regulating volumes is influenced by the decision of regulating power offers. Closing these research gaps by incorporating uncertainty considerations, particularly in the context of activated regulating volumes, will contribute to a more comprehensive understanding of the optimal offering and operation of HPPs in VBMs.

Therefore, this paper proposes a two-level robust optimization framework for look-ahead optimal offering and operation of hybrid wind-battery plants (HWBPs) in VBMs. To the best of the author's knowledge, this is the first study to investigate the look-ahead participation of HWBPs in VBMs, considering both DIU and DDU. The contributions are:

- 1) The two-level robust optimal offering and operation framework is proposed. The dependence relationship between regulating power offers and the uncertainty of activated regulating volumes is captured via the novel framework. Besides, the framework also incorporates the state-of-art probabilistic forecasts for wind power [25] and the regulating price uncertainty is modeled by scenarios generated by k-means clustering. Furthermore, an accurate non-linear battery degradation model [26] is incorporated into the model to extend the battery lifetime.

- 2) A nested adaptive column and constraint generation (C&CG) algorithm is customized to solve the proposed framework effectively. In the external adaptive C&CG algorithm, a mapping approach is developed to project the identified vertices into DDU set of master problem. Since the sub-problem is max-min optimization with integral variables, the internal C&CG algorithm is applied to solve the optimization, resulting in nestification. The process involves the big-M method to convert complementary slackness conditions to mixed integral constraints. An adaptive method is introduced to choose tighter M values.

- 3) Through the case studies, this paper finds that without considering the uncertainty of activated regulating volumes leads to aggressive offering strategies of regulating power. Once activated, HPPs cannot guarantee a feasible supply of regulating power, enabling the potential quarantine of HPPs from participating in VBMs.

The rest of this paper is organized as follows. Section II presents mathematical formulations of the proposed robust framework. The quantification of uncertainties is introduced in Section III. An customized nested adaptive C&CG algorithm is developed in Section IV to solve the proposed framework.

TABLE I
 COMPARISONS OF THE RECENT STUDIES ON HPP IN ELECTRICITY MARKETS

Ref. No.	HPP configuration	Market consideration	Uncertainty consideration	Time stage	Modelling method
[8]	Wind+Battery	SM	-	DA	Deterministic optimization
[9]	Wind+ESS	SM+IS	Wind+Price	DA	Stochastic optimization
[10]	Wind+Solar+Battery	SM+IS	Wind+Solar+Price	DA	Stochastic optimization
[11]	Wind+Battery	SM+IS	Wind+Price	DA	Distributionally robust optimization
[12]	Wind+Battery	SM+IS	Wind	DA	Distributionally robust optimization
[13]	Wind+Battery+Other	SM+IDM+IS	Wind+Price	DA	Stochastic/Robust optimization
[14]	Wind+Other	SM+IDM+IS	Wind+Price	DA	Stochastic optimization
[15]	Wind+Battery+Other	SM+IDM+IS	Wind+Price	DA	Stochastic optimization
[16]	Wind+Solar+Battery+Other	SM+IDM+IS	Wind+Solar+Price	DA	Stochastic/Robust optimization
[17]	Wind+Battery	SM+IDM+IS	Wind+Price	DA	Stochastic optimization
[18]	Wind+Solar+ESS	SM+IDM+IS	Wind+Solar+Price	DA	Stochastic optimization
[19]	Wind+Battery	RM+SM	Wind+Price+reserve activation state	DA	Stochastic optimization
[20]	Wind+Other	RM+SM+IS	Wind+Price	DA	Stochastic optimization
[21]	Wind+ESS	RM+SM+IS	Wind+Price+Regulating volumes	DA	Stochastic optimization
[22]	Wind+ESS	RM+SM+IDM+IS	Wind+Price+Regulating volumes	DA	Stochastic optimization
[23]	Wind+Battery	SM+VBM+IS	Wind+Price	HA	Stochastic/Robust optimization
[24]	Wind+Battery	SM+VBM+IS	-	DA+HA	Deterministic optimization
This paper	Wind+Battery	VBM+IS	Wind+Price+Regulating volumes	HA	Robust/Stochastic optimization

Case studies are given in Section V and conclusions are summarized in Section VI.

II. MATHEMATICAL MODELS

A. Objective function

The objective function is to minimize negative profits of HPP over the worst-case wind power forecasting errors scenario. The formulations are given as:

$$\min_{x \in X} \max_{\substack{\xi_t^w \in \mathcal{W} \\ \tilde{P}_t^{up}, \tilde{P}_t^{dw} \in \mathcal{U}(\cdot, \cdot)}} \min_{y \in Y} [F_1(y) + F_2(y) + F_3(y) + F_4(y)]$$

$$F_1(y) = \sum_{s \in \mathcal{S}} q_s \sum_{t \in \mathcal{T}_1} (\beta_{t,s}^{dw} \cdot \tilde{P}_t^{dw} \cdot \Delta t - \beta_{t,s}^{up} \cdot \tilde{P}_t^{up} \cdot \Delta t) \quad (1)$$

$$F_2(y) = \sum_{s \in \mathcal{S}} q_s \sum_{t \in \mathcal{T}_0} (\beta_{t,s}^{up} \cdot \Delta \tilde{P}_t^{dw} \cdot \Delta t - \beta_{t,s}^{dw} \cdot \Delta \tilde{P}_t^{up} \cdot \Delta t) \quad (2)$$

$$F_3(y) = \sum_{t \in \mathcal{T}_0} (C^{im} \cdot |\Delta \tilde{P}_t^{dev}| \cdot \Delta t) \quad (3)$$

$$F_4(y) = \sum_{t \in \mathcal{T}_0} [C^{deg} \cdot (\tilde{P}_t^{dis} + \tilde{P}_t^{cha}) \cdot \Delta t] \quad (4)$$

where $\mathcal{U}(\cdot, \cdot)$ and \mathcal{W} represent the DDU and DIU sets, respectively. $F_1(x)$, $F_2(y)$ are negative expected revenues from providing balancing service and negative expected revenues from imbalance settlement under the two-price model [27], respectively. $\beta_{t,s}^{up}$ and $\beta_{t,s}^{dw}$ are the scenario of up and down balancing price, respectively. They are calculated by:

$$\beta_{t,s}^{up} = \begin{cases} \pi_{t,s}^{rp}, & \text{if } \pi_{t,s}^{rp} \geq \pi_t^{sp} \\ \pi_t^{sp}, & \text{otherwise} \end{cases} \quad (5)$$

$$\beta_{t,s}^{dw} = \begin{cases} \pi_{t,s}^{rp}, & \text{if } \pi_{t,s}^{rp} \leq \pi_t^{sp} \\ \pi_t^{sp}, & \text{otherwise} \end{cases} \quad (6)$$

$F_3(y)$ denotes costs of power deviation from the most recently updated generation plan, where C^{im} is the deviation cost per MWh. This cost comes from the fact that in European countries, there are legal or contractual requirements for power plants to track their most recently updated generation plan

[28]. It is noted that $F_3(y)$ has absolute item, which can be transferred as (7a)-(7c) by introducing an auxiliary variable τ_t .

$$F_3(y) = \sum_{t \in \mathcal{T}_0} (C^{im} \cdot \tau_t \cdot \Delta t) \quad (7a)$$

$$\tau_t \geq \Delta \tilde{P}_t^{dev} \quad (7b)$$

$$\tau_t \geq -\Delta \tilde{P}_t^{dev} \quad (7c)$$

$F_4(y)$ represents costs of battery degradation, where C^{deg} is the cost of degradation per MWh energy throughput. The value is estimated from an accurate non-linear battery degradation model [26] and varies every day in order to represent the non-linear degradation process. Detailed information of calculating C^{deg} refers to [24]. X and Y are the first-level and second-level constraints introduced in the following parts.

B. First-level constraints

1) *Look-ahead operation constraints*: The optimization horizon \mathcal{T}_0 is always from the current time period t_0 to the end of the day. Therefore, $\forall t \in \mathcal{T}_0$:

$$P_t^{ha} = P_t^w + P_t^{dis} - P_t^{cha} \quad (8a)$$

$$0 \leq P_t^{dis} \leq P^{b,max} \cdot z_t \quad (8b)$$

$$0 \leq P_t^{cha} \leq P^{b,max} \cdot (1 - z_t) \quad (8c)$$

$$E_{t+1}^b = E_t^b(1 - \eta_l) - \frac{P_t^{dis}}{\eta_{dis}} \cdot \Delta t - P_t^{cha} \cdot \eta_{cha} \cdot \Delta t \quad (8d)$$

$$E^{min} \leq E_{t+1}^b \leq E^{max} \quad (8e)$$

$$P_t^{ha} + P_t^{up,*} \leq P^{grid}, \quad \forall t \in \mathcal{T}_0 \setminus \mathcal{T}_1 \quad (8f)$$

$$P_t^{ha} + P_t^{up} \leq P^{grid}, \quad \forall t \in \mathcal{T}_1 \quad (8g)$$

$$P_t^{ha} - P_t^{dw,*} \geq 0, \quad \forall t \in \mathcal{T}_0 \setminus \mathcal{T}_1 \quad (8h)$$

$$P_t^{ha} - P_t^{dw} \geq 0, \quad \forall t \in \mathcal{T}_1 \quad (8i)$$

$$E_t^b = E_{t_0}, \quad \forall t = t_0 \quad (8j)$$

where $P_t^{up,*}$ and $P_t^{dw,*}$ are the known regulating power offer. \mathcal{T}_1 is the offering horizon. The reason to distinguish the optimization horizon and the offering horizon is that at the time of running the proposed model, at least the regulating power offer of the current hour is fixed. Constraints (8a)-(8e), and (8j) are common operation constraints for power balance, discharging and charging the battery, battery evolution, battery

energy limitation, and battery initial energy. Since HPPs are normally overplanted, constraints (8f) and (8g) restrict that the maximum possible HPP power output should not exceed grid connection capacity due to the overplanting of the HPP with regards to grid connection capacity. Besides, constraints (8h) and (8i) restrict that the HPP is a power supplier rather than a power consumer.

2) *Look-ahead offering constraints*: At the time of implementing optimization, the gate of balancing market for period t_0 is closed. Hence, the offering constraints are only valid for \mathcal{T}_1 , starting from t_1 to the end of the day. Therefore, $\forall t \in \mathcal{T}_1$:

$$P_t^w + P_t^{w,up} \leq P^{w,max} \quad (9a)$$

$$P_t^w - P_t^{w,dw} \geq 0 \quad (9b)$$

$$P_t^{dis} - P_t^{cha} + P_t^{b,up} \leq P^{b,max} \quad (9c)$$

$$P_t^{dis} - P_t^{cha} - P_t^{b,dw} \geq -P^{b,max} \quad (9d)$$

$$P_t^{up} = P_t^{w,up} + P_t^{b,up} \quad (9e)$$

$$P_t^{dw} = P_t^{w,dw} + P_t^{b,dw} \quad (9f)$$

$$P_t^{up} \leq P^{up,max} \quad (9g)$$

$$P_t^{dw} \leq P^{dw,max} \quad (9h)$$

$$P_t^{up} = 0 \vee P_t^{up} \geq P^{up,min} \quad (9i)$$

$$P_t^{dw} = 0 \vee P_t^{dw} \geq P^{dw,min} \quad (9j)$$

Constraint (9a) restricts the planned wind power output, including up regulating offer from wind power that is less than rated power capacity, while constraint (9b) limits the planned wind power output, including down regulating offer from wind power that is greater than 0. Similar constraints (9c) and (9d) are applied for battery. Constraints (9e) and (9f) describe the relationship between the total up/down regulating power and up/down regulating power from individual technologies. Constraints (9g) and (9h) give the maximum volumes for up and down regulating power offer. Constraints (9i) and (9j) indicate that the HPP either does not offer the regulating power or offers regulating power greater than the minimum requirements. Note that this is for the HPP who does not commit balancing capacity in the DA RM. However, if the HPP has participated in the DA RM, the regulating power offer must be higher than the committed balancing capacity. It is noted that (9i) and (9j) can be linearized as mixed integral linear constraints using big M method according to [19], given as:

$$-M_1 \cdot (1 - z_t^{up}) \leq P_t^{up} \leq M_1 \cdot (1 - z_t^{up}) \quad (10a)$$

$$P^{up,min} - M_1 \cdot z_t^{up} \leq P_t^{up} \quad (10b)$$

$$-M_2 \cdot (1 - z_t^{dw}) \leq P_t^{dw} \leq M_2 \cdot (1 - z_t^{dw}) \quad (10c)$$

$$P^{dw,min} - M_2 \cdot z_t^{dw} \leq P_t^{dw} \quad (10d)$$

$$z_t^{up}, z_t^{dw} \in \{0, 1\} \quad (10e)$$

The big M values, M_1 and M_2 , can be chosen as $P^{up,max}$, $P^{dw,max}$, respectively.

C. Second-level constraints

1) *Real-time operation constraints*: The variables in second-level are all uncertainty dependent variables with the symbol $\tilde{\cdot}$. In real-time, the HPP, wind, and battery should

meet the following physical constraints, which have similar meanings as first-level operation constraints.

$$\tilde{P}_t^{rt} = \tilde{P}_t^w + \tilde{P}_t^{dis} - \tilde{P}_t^{cha} \quad (11a)$$

$$0 \leq \tilde{P}_t^{dis} \leq P^{b,max} \cdot \tilde{z}_t \quad (11b)$$

$$0 \leq \tilde{P}_t^{cha} \leq P^{b,max} \cdot (1 - \tilde{z}_t) \quad (11c)$$

$$\tilde{E}_{t+1}^b = \tilde{E}_t^b(1 - \eta_l) - \frac{\tilde{P}_t^{dis}}{\eta_{dis}} \cdot \Delta t - \tilde{P}_t^{cha} \cdot \eta_{cha} \cdot \Delta t \quad (11d)$$

$$E^{min} \leq \tilde{E}_{t+1}^b \leq E^{max} \quad (11e)$$

$$0 \leq \tilde{P}_t^{rt} \leq P^{grid} \quad (11f)$$

$$0 \leq \tilde{P}_t^w \leq \tilde{P}_t^{ava,w} \quad (11g)$$

$$\tilde{E}_t^b = E_{t_0}^b, \quad \forall t = t_0 \quad (11h)$$

2) *Day-after imbalance settlement constraints*: The imbalance settlement consists of two parts: 1) the settlement of energy imbalance from SM energy plan; 2) the settlement of power deviation from the most recently updated power plan.

$$\Delta \tilde{P}_t = \tilde{P}_t^{rt} - P_t^{sm} - \tilde{P}_t^{up} + \tilde{P}_t^{dw} \quad (12a)$$

$$\Delta \tilde{P}_t = \Delta \tilde{P}_t^{up} - \Delta \tilde{P}_t^{dw} \quad (12b)$$

$$\Delta \tilde{P}_t^{up} \cdot \Delta \tilde{P}_t^{dw} = 0 \quad (12c)$$

$$\Delta \tilde{P}_t^{up}, \Delta \tilde{P}_t^{dw} \geq 0 \quad (12d)$$

$$\Delta \tilde{P}_t^{dev} + \tilde{P}_t^{up} - \tilde{P}_t^{dw} = \tilde{P}_t^{rt} - P_t^{ha} \quad (12e)$$

Constraint (12a) calculates imbalance power, which is the difference between the real-time power output and promised power in spot market as well as promised regulating power in balancing market. Constraint (12b) divides the imbalance power into positive and negative imbalance power, which are constrained by (12c) and (12d). Note that (12c) is bi-linear constraint, which can also be linearized by big M method, expressed as:

$$\Delta \tilde{P}_t^{up} \leq M_3 \cdot z_t^\Delta \quad (13a)$$

$$\Delta \tilde{P}_t^{dw} \leq M_3 \cdot (1 - z_t^\Delta) \quad (13b)$$

$$z_t^\Delta \in \{0, 1\} \quad (13c)$$

The big M values, M_3 , can be chosen as P^{grid} .

Constraint (12e) calculates the power deviation between real-time power output and look-ahead power plan as well as the activated regulating power in balancing markets.

III. UNCERTAINTY QUANTIFICATION

A. Quantify uncertainty of activated regulating power

The activated up and down regulating power, denoted as $\tilde{P}_t^{up}, \tilde{P}_t^{dw}$, depends on look-ahead up and down regulating power offers P_t^{up}, P_t^{dw} . The uncertainty set $\mathcal{U}(P_t^{up}, P_t^{dw})$ can be defined as:

$$\mathcal{U}(P_t^{up}, P_t^{dw}) = \left\{ (\tilde{P}_t^{up}, \tilde{P}_t^{dw}) \left| \begin{array}{l} \tilde{P}_t^{up} = 0 \vee P_t^{up} \\ \tilde{P}_t^{dw} = 0 \vee P_t^{dw} \\ \tilde{P}_t^{up} \cdot \tilde{P}_t^{dw} = 0 \end{array} \right. \right\} \quad (14)$$

The initial two equations impose constraints on the activated regulating power, ensuring that it is either zero or equal to the maximum offer. The non-linear constraint $\tilde{P}_t^{up} \cdot \tilde{P}_t^{dw} = 0$ lies in the fact that in each activation interval, either up or down

regulating power can be activated. All these constraints can be linearized as:

$$\tilde{P}_t^{up} \leq M_4 \cdot \hat{z}_t^{up} \quad (15a)$$

$$\tilde{P}_t^{up} \geq -M_4 \cdot (1 - \hat{z}_t^{up}) + P_t^{up} \quad (15b)$$

$$\tilde{P}_t^{dw} \leq M_5 \cdot \hat{z}_t^{dw} \quad (15c)$$

$$\tilde{P}_t^{dw} \geq -M_5 \cdot (1 - \hat{z}_t^{dw}) + P_t^{dw} \quad (15d)$$

$$\tilde{P}_t^{up} \leq M_6 \cdot \hat{z}_t \quad (15e)$$

$$\tilde{P}_t^{dw} \leq M_6 \cdot (1 - \hat{z}_t) \quad (15f)$$

$$\hat{z}_t^{up}, \hat{z}_t^{dw}, \hat{z}_t \in \{0, 1\} \quad (15g)$$

The advantage of employing the DDU set is its independence from any prior information regarding activated regulating volumes. This becomes particularly valuable in situations where there is limited or insufficient data available about the probabilistic distribution of activated regulating volumes.

B. Quantify the uncertainty of wind power

The uncertainty of wind power is described using the box uncertainty set, denoted as:

$$\mathcal{W} := \{\tilde{P}_t^{ava,w} | \underline{P}_t^{ava,w} \leq \tilde{P}_t^{ava,w} \leq \overline{P}_t^{ava,w}\} \quad (16)$$

where $\underline{P}_t^{ava,w}$ and $\overline{P}_t^{ava,w}$ are the lower and upper bound of the available wind power at the plant level. The bounds are obtained using the quantile regression forest (QRF) model, which is a well-established probabilistic model for wind power forecasting [29] and ranks among the best-performing forecasting methods [30]. The framework presented in [31] is used to generate the probabilistic forecasts. The following paragraphs will briefly describe the methodologies used, and the interested reader is referred to [31] for a more in depth explanation of the probabilistic forecasting framework.

The QRF model is used to post-process numerical weather prediction forecasts. Hub height wind speed were at the grid point closest to the wind park from the freely available Meteorological Cooperation on Operational Numeric Weather Prediction (MetCoOp) from the Norwegian meteorological institute [32] (12 UTC cycle runs, lead times $t + k, k \in \{12, 13, \dots, 36\}$) and 24 hour time lagged power observations are used as explanatory variables to train and test the QRF models. Learning the QRF model is mainly influenced by three hyperparameters; the number of variables to randomly select from (*max_features*) the minimum number of trees (*n_estimators*) and the minimum number of observations in each leaf (*min_samples_leaf*). The number of variables to select from is set to 1/3 of the available variables, the number of trees are set to 1000 and the minimum number of observations per leaf is set to 10 to avoid overfitting. Since wind production behaved differently according to the forecast horizon, e.g. diurnal variability, one QRF model is trained for each forecast horizon.

It was found in [31] that the reliability, which is a desired property when trading using probabilistic production forecasts, was not sufficient with solely using the QRF models. Therefore, the QRF forecasts were post-processed using quantile regression (QR) [33]. The QR model produces a non-parametric cumulative distribution function by assuming a linear relationship between the QRF forecast distributions and the observations. From the QR model, forecasts with 19 evenly spaced nominal probabilities, $\tau \in \{0.05, \dots, 0.95\}$, were produced and used for optimization model evaluation.

C. Quantify the uncertainty of regulating price

The uncertainty of regulating price is represented by a set of scenarios. At the time of offering, the spot price is known. To utilize this information, the scenarios of regulating prices are generated with the following steps:

Step 1: The historical spot prices and the spot prices of the operation day are clustered using k-means clustering [34].

Step 2: Identify the cluster which contains the spot prices of the operation day and record the indices of the historical days in this cluster.

Step 3: The regulating prices corresponding to the indices of the historical days are clustered using k-means clustering again. Then each centroid of new clusters is the scenario of regulating prices.

IV. SOLUTION ALGORITHM

The proposed two-level robust optimization model has two special features: 1) It contains the DDU set; 2) The recourse problem is a mixed integral linear programming (MILP). These two features make it difficult for the traditional C&CG algorithm [35] to solve the proposed model. The reasons are that identified vertices from subproblems may be infeasible for the new DDU set in each iteration [36] and Karush–Kuhn–Tucker (KKT) conditions do not hold for MILP. Therefore, this paper proposes a NAC&CG algorithm to solve the proposed model based on [36] and [37].

A. Solving subproblem

The subproblem (\mathcal{SP}) is defined as follows:

$$\mathcal{SP} : \max_{\substack{\tilde{\xi}_t^w \in \mathcal{W} \\ \tilde{P}_t^{up}, \tilde{P}_t^{dw} \in \mathcal{U}(\cdot, \cdot)}} \min_{y_1, y_2, z} a^T \cdot y_1 + b^T \cdot y_2 \quad (17a)$$

$$s.t. \quad y_1, y_2, z \in \mathcal{Y}(x_k^*, \tilde{P}_t^{up}, \tilde{P}_t^{dw}, \tilde{\xi}_t^w) \quad (17b)$$

$$y_1 \geq 0, z \in \{0, 1\} \quad (17c)$$

where x_k^* is the optimal solution of the master problem during iteration k ; a, b are coefficients in the objective function; y_1, y_2 and z represent second-level variables defined as:

$$y_1 := \{\tilde{P}_t^{rt}, \tilde{P}_t^w, \tilde{P}_t^{dis}, \tilde{P}_t^{cha}, \Delta \tilde{P}_t^{up}, \Delta \tilde{P}_t^{dw}, \tilde{P}_t^{map,up}, \tilde{P}_t^{map,dw}\}$$

$$y_2 := \{\tilde{\Delta} P_t, \tilde{\Delta} P_t^{spc}, \tilde{E}_t^b, \tilde{\tau}_t\}$$

$$z := \{\tilde{z}_t, \tilde{z}_t^\Delta\}$$

and $\mathcal{Y}(x_k^*, \tilde{P}_t^{up}, \tilde{P}_t^{dw}, \tilde{\xi}_t^w) := \{(11a) - (13c)\}$ represent second-level constraints, which have the compact form:

$$A_1 x_k^* + B_1 y_1 + C_1 y_2 + D_1 z + E_1 \cdot \tilde{P}^{up} + G_1 \cdot \tilde{P}^{dw} + H_1 \cdot \tilde{\xi}^w + f_1 \leq 0 \quad (18a)$$

$$A_2 x_k^* + B_2 y_1 + C_2 y_2 + E_2 \cdot \tilde{P}^{up} + G_2 \cdot \tilde{P}^{dw} + H_2 \cdot \tilde{\xi}^w + f_2 = 0 \quad (18b)$$

where $A_1, A_2, B_1, B_2, C_1, C_2, D_1, E_1, E_2, G_1, G_2, H_1, H_2, f_1, f_2$ are coefficients of the constraints.

\mathcal{SP} is a max-min problem with integral variables existing in the inner minimization problem. Therefore, it cannot be directly converted using KKT conditions. Instead, according to

[37], by separating integral variable z and continuous variable y , \mathcal{SP} can be reformulated as:

$$\max_{\tilde{\xi}_t^w, \tilde{P}_t^{up}, \tilde{P}_t^{dw}} \min_z \min_{y_1, y_2} a^T \cdot y_1 + b^T \cdot y_2 \quad (19a)$$

$$s.t. \quad y_1, y_2, z \in \mathcal{Y}(x_k^*, \tilde{P}_t^{up}, \tilde{P}_t^{dw}, \tilde{\xi}_t^w) \quad (19b)$$

$$\tilde{\xi}_t^w \in \mathcal{W} \quad (19c)$$

$$\tilde{P}_t^{up}, \tilde{P}_t^{dw} \in \mathcal{U}(\tilde{P}_t^{up}, \tilde{P}_t^{dw}) \quad (19d)$$

$$y_1 \geq 0, z \in \{0, 1\} \quad (19e)$$

Then, the classical C&CG algorithm [35] can accommodate the above optimization. Hence, the sub-sub-problem (\mathcal{SSP}) is defined as:

$$\mathcal{SSP} : \min_{y_1, y_2, z} a^T \cdot y_1 + b^T \cdot y_2 \quad (20a)$$

$$s.t. \quad y_1, y_2, z \in \mathcal{Y}(x_k^*, \tilde{P}_{t,l}^{up,*}, \tilde{P}_{t,l}^{dw,*}, \tilde{\xi}_{t,l}^{w,*}) \quad (20b)$$

$$y_1 \geq 0, z \in \{0, 1\} \quad (20c)$$

where $\tilde{P}_{t,l}^{up,*}, \tilde{P}_{t,l}^{dw,*}, \tilde{\xi}_{t,l}^{w,*}$ are the optimal solution of sub-master problem \mathcal{SMP} during iteration l .

Assume that the optimal solution of \mathcal{SSP} is z_l^* , the \mathcal{SMP} can be defined as:

$$\mathcal{SMP} : \max_{\tilde{\xi}_t^w, \tilde{P}_t^{up}, \tilde{P}_t^{dw}} \eta_1 \quad (21a)$$

$$s.t. \quad \tilde{\xi}_t^w \in \mathcal{W}, \quad (21b)$$

$$\tilde{P}_t^{up}, \tilde{P}_t^{dw} \in \mathcal{U}(P_t^{up}, P_t^{dw}) \quad (21c)$$

$$\eta_1 \leq \min a^T \cdot y_{1,l+1} + b^T \cdot y_{2,l+1} \quad (21d)$$

$$A_1 x_k^* + B_1 y_{1,l+1} + C_1 y_{2,l+1} + D_1 z_l^* + E_1 \cdot \tilde{P}^{up} + G_1 \cdot \tilde{P}^{dw} \quad (21e)$$

$$+ H_1 \cdot \tilde{\xi}^w + f_1 \leq 0$$

$$A_2 x_k^* + B_2 y_{1,l+1} + C_2 y_{2,l+1} + E_2 \cdot \tilde{P}^{up} + G_2 \cdot \tilde{P}^{dw} \quad (21f)$$

$$+ H_2 \cdot \tilde{\xi}^w + f_2 = 0$$

$$y_{1,l+1} \geq 0 \quad (21g)$$

$$\forall l \in \mathcal{L} \quad (21h)$$

Note that constraints (21d)-(21g) contain a minimization problem, which is a linear programming. The KKT conditions can be utilized to convert it into a feasibility problem. Specifically, let λ , μ , and v be the dual variables of the constraint (21e)-(21g), respectively. The minimization problem is equivalent to the following KKT equations:

$$A_1 x_k^* + B_1 y_{1,l+1} + C_1 y_{2,l+1} + D_1 z_l^* + E_1 \cdot \tilde{P}^{up} + G_1 \cdot \tilde{P}^{dw} + H_1 \cdot \tilde{\xi}^w + f_1 \leq 0 \quad (22a)$$

$$A_2 x_k^* + B_2 y_{1,l+1} + C_2 y_{2,l+1} + E_2 \cdot \tilde{P}^{up} + G_2 \cdot \tilde{P}^{dw} + H_2 \cdot \tilde{\xi}^w + f_2 = 0 \quad (22b)$$

$$B_1^T \lambda + B_2^T \mu + a \geq 0 \quad (22c)$$

$$\lambda_i \cdot (A_1 x_k^* + B_1 y_{1,l+1} + C_1 y_{2,l+1} + D_1 z_l^* + E_1 \cdot \tilde{P}^{up} + G_1 \cdot \tilde{P}^{dw} + H_1 \cdot \tilde{\xi}^w + f_1)_i = 0 \quad (22d)$$

$$y_{1,l+1,i} \cdot (B_1^T \lambda + B_2^T \mu + a)_i = 0 \quad (22e)$$

$$C_1^T \lambda + C_2^T \mu + b = 0 \quad (22f)$$

$$\lambda \geq 0, y_{1,l+1} \geq 0 \quad (22g)$$

where variables and equations with subscript i represents the i^{th} element. (22d) and (22e) are complementary slackness conditions, which have the equivalent mixed integral formulations as follows:

$$\lambda_i \leq M_7 \cdot (1 - z_i^\lambda) \quad (23a)$$

$$(A_1 x_k^* + B_1 y_{1,l+1} + C_1 y_{2,l+1} + D_1 z_l^* + E_1 \cdot \tilde{P}^{up} + G_1 \cdot \tilde{P}^{dw} + H_1 \cdot \tilde{\xi}^w + f_1)_i \geq M_8 \cdot z_i^\lambda \quad (23b)$$

$$y_{1,l+1,i} \leq M_9 \cdot (1 - z_i^y) \quad (23c)$$

$$(B_1^T \lambda + B_2^T \mu + a)_i \leq M_{10} \cdot z_i^y \quad (23d)$$

where M_8 and M_{10} can be chosen based on the physical constraints. The big M for dual variables, i.e. M_7 and M_9 has significant impacts the performance of the algorithm. Too large value causes numerical instability, while too small value leads to local optimality or even infeasibility. This paper proposes an adaptive method to select tighter big M for dual variables. The details are introduced in **Appendix A**.

B. Solving master problem

During each iteration k , the master problem (\mathcal{MP}) is defined as follows.

$$\mathcal{MP} : \min_x \eta \quad (24a)$$

$$s.t. \quad x \in \mathcal{X} \quad (24b)$$

$$y_{1,k}, y_{2,k}, z_k \in \mathcal{Y}(x, \tilde{P}_{t,k}^{map,up}, \tilde{P}_{t,k}^{map,dw}, \tilde{\xi}_{t,k}^{w,*}) \quad (24c)$$

$$\eta \geq a^T \cdot y_k, \quad (24d)$$

$$\tilde{P}_{t,k}^{map,up} = P_t^{up} \cdot \hat{z}_{t,k}^{up,*}, \quad (24e)$$

$$\tilde{P}_{t,k}^{map,dw} = P_t^{dw} \cdot \hat{z}_{t,k}^{dw,*}, \quad (24f)$$

$$\forall k \in \mathcal{N}, z_k \in \{0, 1\} \quad (24g)$$

where x is first-level decision variables denoted as $x := \{P_t^w, P_t^{dis}, P_t^{cha}, P_t^{up}, P_t^{dw}, P_t^{up,w}, P_t^{dw,w}, P_t^{up,b}, P_t^{dw,b}\}$. \mathcal{X} is first-level constraints denoted as $\mathcal{X} := \{(8a) - (9h), (10a) - (10e)\}$. y_k, z_k are generated variables, while constraints (24c) and (24d) are generated constraints. (24e) and (24f) are constraints to project the identified vertices from the k^{th} uncertainty set $\mathcal{U}_k(P_{t,k}^{up}, P_{t,k}^{dw})$ into the new DDU set.

C. Nested adaptive C&CG algorithm

The overall process of the NAC&CG algorithm is summarized in **Algorithm 1**. For simplification, the time index t in the following algorithms is omitted.

Algorithm 1 NAC&CG algorithm

- 1: **Initialize:** Accuracy tolerance $\epsilon \geq 0$; Iteration index $k = 1$; Upper bound $UB_0 = 10^{10}$; Lower bound $LB_0 = -10^{10}$; Worst scenario set $\mathcal{N} = \emptyset$.
 - 2: **while** k **do**
 - 3: **Master problem:** Solve the \mathcal{MP} and obtain the optimal solution x_k^* . Update the lower bound $LB_k = \eta^k$.
 - 4: **Sub-problem:** Solve the \mathcal{SP} using **Algorithm 2** and obtain the worst-case $\omega_k^* = (\tilde{\xi}_k^{w,*}, \tilde{P}_k^{up,*}, \tilde{P}_k^{dw,*})$. Update the upper bound $UB_k = \min\{UB_{k-1}, a^T \cdot y_{1,k}^* + b^T \cdot y_{2,k}^*\}$.
 - 5: **Termination condition:** If $|UB_k - LB_k| \leq \epsilon$, **break**; Otherwise, $\mathcal{N} = \mathcal{N} \cup \{\omega_k^*\}$ and $k = k + 1$.
 - 6: **end while**
-

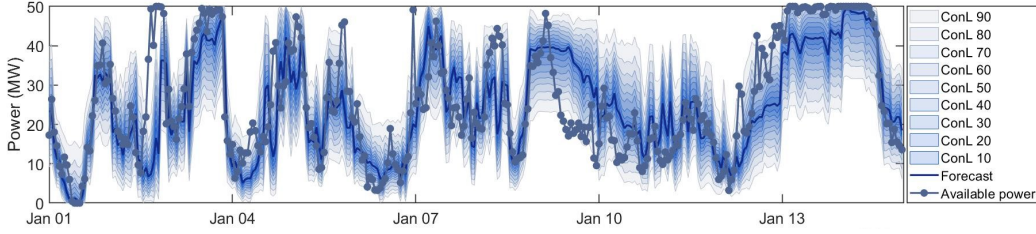


Fig. 2. Probabilistic forecast of wind power

Algorithm 2 Internal C&CG algorithm

- 1: **Initialize:** Accuracy tolerance $\epsilon \geq 0$; Iteration index $l = 1$; Upper bound $UB_0 = 10^{10}$. Lower bound $LB_k = -10^{10}$; Worst scenario set \mathcal{L}
 - 2: **while** 1 **do**
 - 3: **Sub-Master-problem:** Solve the SMP and obtain the optimal solution $(\xi_{k,l}^{w,*}, \bar{P}_{k,l}^{up,*}, \bar{P}_{k,l}^{dw,*})$. Update the upper bound $UB_l = \eta^l$.
 - 4: **Sub-Sub-problem:** Solve the SSP and obtain the worst-case $z_{k,l}^*$. Update the lower bound $LB_l = \min\{LB_{l-1}, a^T \cdot y_{1,k,l}^* + b^T \cdot y_{2,k,l}^*\}$.
 - 5: **Termination condition:** If $|UB_l - LB_l| \leq \epsilon$, **break**; Otherwise, $\mathcal{L} = \mathcal{L} \cup \{z_{k,l}^*\}$ and $l = l + 1$.
 - 6: **M values:** Obtain the tighter M values of dual variables for SMP according to **Appendix A**.
 - 7: **end while**
-

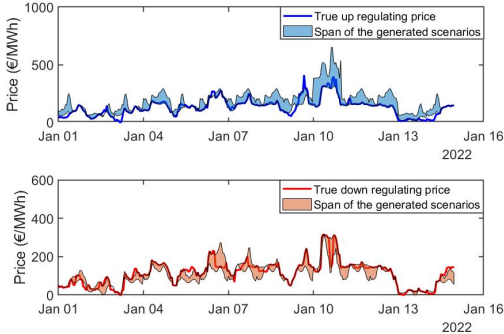


Fig. 3. Scenarios of regulating price

The **Algorithm 1** summarizes the alternative solving of MP and SP . The main differences with traditional C&CG are the including of mapping constraints (24e) and (24f) into MP and applying **Algorithm 2** to solve SP . The global convergence can refer to [36]. In **Algorithm 2**, if the algorithm does not stop at step 5, step 6 is introduced to choose tighter M values. The details can be found in **Appendix A**.

V. CASE STUDIES

The considered HWBP, consisting of a 50 MW wind farm and 10MW/30MWh battery, is assumed to be located in Western Denmark. Correlated renewable energy source tool [38], [39] is applied to simulate wind power generation from 2018 to 2022. The market prices and regulating volumes of Nordic areas from 2021 to 2022 are downloaded on the European Network of Transmission System Operators for Electricity website [40]. These data are applied to obtain probabilistic

forecasts of wind power and scenarios of regulating prices. All case studies are implemented by Python [41] and optimizations are solved using IBM Decision Optimisation Studio CPLEX through the docplex python library [42] operating on DTU's high-performance computing cluster *Sophia* [43].

Figures 2 and 3 display the probabilistic forecasts of wind power and the scenarios of regulating prices, respectively. There are total of 9 confidence levels for wind power and 4 scenarios for regulating prices. In Figure 2, it is evident that the actual wind power aligns closely with the 90% confidence level range, showcasing the effectiveness of the probabilistic forecasts in capturing the inherent variability and uncertainty of wind power. Similarly, in Figure 3, the ranges for both upward and downward regulating power almost encompass the real prices, providing a robust representation of the potential uncertainty in regulating prices. It is important to note that while there are instances where the real values lie outside the depicted ranges, the overall coverage of the forecasts and scenarios accurately captures the majority of the observed variations in wind power and regulating prices.

A. Comparison with Benchmark model

A benchmark model is employed to test the performance of the proposed model. The benchmark model represents the proposed model excluding the consideration of the uncertainty of activated regulating volumes. This involves removing the DDU set $\mathcal{U}(P_t^{up}, P_t^{dw})$ from the objective function (1) and replacing the stochastic variables \bar{P}_t^{up} and \bar{P}_t^{dw} with P_t^{up} and P_t^{dw} , respectively. In the benchmark model, it is assumed that all the offered regulating power is activated in real-time, which aligns with common assumptions found in the literature, such as [23], [24]. It is noted that in the proposed model and the benchmark model, the confidence level of wind power forecasts is chosen as 50%. The consecutive 14 days results of the benchmark model and the proposed model are demonstrated in Fig. 4 and Fig. 5, respectively. In the presented simulation results, the regulating power offers of both models are updated once at 12:00 of the operation day.

The disparity between the benchmark model and the proposed model in terms of the robustness of regulating power offerings is evident in Fig. 4 and Fig. 5. Nearly every hour, as shown in the upper figure of Figure. 4, the benchmark model tends to offer regulating power, which indicates a relatively aggressive offering strategy. Consequently, as demonstrated in the lower figure of Figure. 4, the HPP with the benchmark model faces challenges in adhering to the committed reference in 11 hours, resulting in deviations from their initial power commitments. In contrast, the proposed model offers a reduced amount of regulating power in the market. For example, as depicted in the upper figure of Figure. 5, during the end of Jan 03 and the beginning of Jan 04, there is no regulating power offering, indicating a more cautious offering strategy.

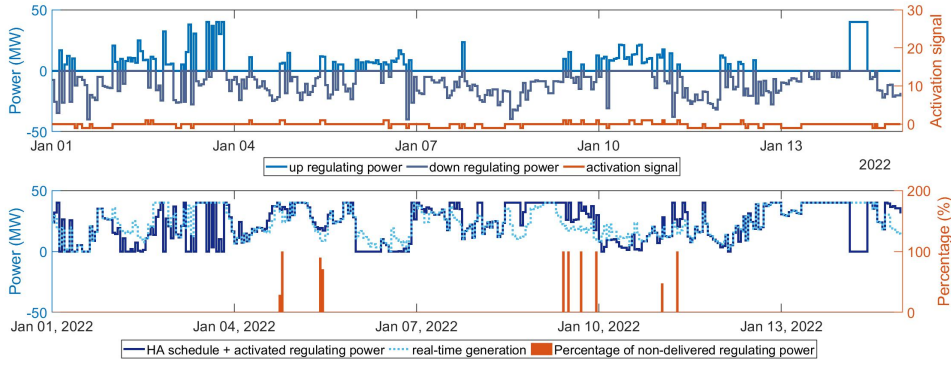


Fig. 4. Results of the benchmark model

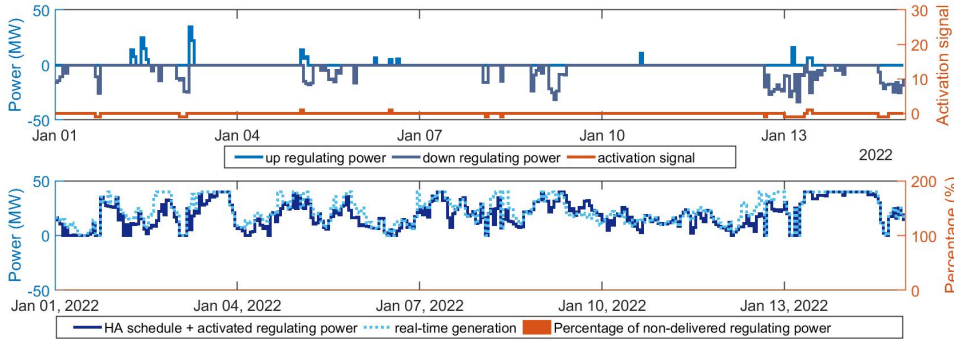


Fig. 5. Results of the proposed model

However, for the HPP with the proposed model, when regulating power offers are activated, the HPP consistently delivers the required power as expected.

B. Impact of confidence levels of probabilistic wind power forecasts

This section investigates how confidence levels of probabilistic wind power forecasts affect the performance of the benchmark model and the proposed model. The statistics of the count and the percentage of hours during which the HPP fails to provide balancing service per the TSO's request are shown in Table. II, where 5 confidence levels are considered. It is observed in Table. II that the number of hours decreases for both models as the confidence level rises. This is because of the inclusion of more extreme wind power scenarios in the uncertainty set when higher confidence levels are considered. As a result, both models adopt more robust decisions to ensure reliable operation in the face of uncertainty. Despite considering a 90% confidence level, there are still 5 hours in which the benchmark model fails to deliver the committed regulating power. It occupies around 6% of the total number of hours that the regulating power is activated. Consequently, there is a risk of the HPP being excluded by the TSO from providing balancing services. However, the proposed model demonstrates its capability to fully deliver the committed regulating power when the confidence level surpasses 30%. This highlights the improved performance and reliability of the proposed model.

Furthermore, Table III provides a detailed comparison of the HPP's profitability using the proposed model at different confidence levels. Notably, higher confidence levels lead to

TABLE II
THE COUNT AND PERCENTAGE OF HOURS DURING WHICH THE HPP FAILS TO PROVIDE BALANCING SERVICE PER THE TSO'S REQUEST

Model	Confidence level	Number of hours	Percentage
Benchmark model	10%	21	22%
	30%	17	18%
	50%	10	11%
	70%	6	7%
	90%	5	6%
The proposed model	10%	3	15%
	30%	3	15%
	50%	0	0%
	70%	0	0%
	90%	0	0%

more conservative decisions, i.e. fewer regulating power offers, which in turn affects the variations in revenues and costs as shown in the table.

Firstly, as the confidence levels increase, the regulation revenue rises from -15.5 k€ to -14.8 k€. This could be attributed to the decrease in the provision of down-regulating power, leading to lower payments for down-balancing services. However, the energy imbalance cost, caused by the imbalance energy ΔP , increases from 121.3 k€ to 136.8 k€, and the power imbalance cost, caused by the power deviation ΔP^{dev} , increases from 4.1 k€ to 12.6 k€. The reason for these increases is that the opportunities to reduce the imbalance costs by offering the imbalances as regulating power are reduced. On the other hand, the battery degradation costs decrease as the battery is less frequently utilized with fewer balancing service provisions. Additionally, since fewer regulating power

TABLE III
REVENUES AND COSTS (THOUSAND €) COMPARISON OF THE PROPOSED MODEL AT DIFFERENT CONFIDENCE LEVELS

Confidence level	SM revenues	BM revenues			Total revenues	Degradation costs	Total profits	
		regulation revenues	energy imbalance costs	power imbalance costs				
50%	966.7	-15.5	121.3	4.1	-140.9	825.8	12.9	812.9
70%	969.2	-15.2	127.9	6.8	-148.9	820.3	11.5	808.9
90%	972.2	-14.8	136.8	12.6	-163.1	809.1	10.1	799.0

offers lead to more energy stored in batteries, more energy in batteries can be used for spot market offerings daily. Consequently, the spot market revenue also increases with a higher confidence level.

Taking these trade-offs into account, the maximum total profits are achieved at the 50% confidence level. This indicates that selecting a confidence level of 50% represents a well-balanced trade-off between economic performance and the robustness of the proposed model.

C. Performance of the proposed NAC&CG algorithm

The computational performance of the proposed model is demonstrated in Fig. 6. The notation "22:00, D-1" indicates that the model is executed at 22:00 on the previous day, while "12:00, D" implies that the regulating power offers are updated at 12:00 on the operation day. The figure showcases the solving time for the model when run twice, with solving times ranging from 348s to 2263s for the first run and from 8s to 875s for the second run. The solving times of the proposed model are deemed acceptable. For instance, considering that the first offer needs to be submitted by 23:15, D-1, allowing a time window of 4500s between 22:00 and 23:15. Remarkably, the maximum solving time of 2263s comfortably fits within this time frame. Similarly, for the second run, the maximum solving time of 875 seconds is well below the 900 seconds time window between 12:00 and 12:15. In fact, users have the flexibility to choose their preferred execution time of the proposed model, enabling them to submit or modify their regulating power offers well ahead of the deadline. It is important to note that the computational performance of the model is dependent on the worst-case scenario, which accounts for the wide time range observed. Additionally, it is reasonable that the average solving time for the second run (254s) is lower than the first run (1408s) since the optimization horizon is reduced during the second run.

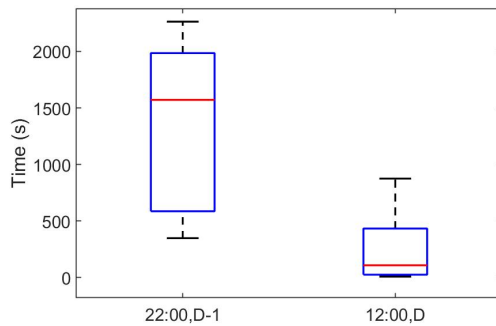


Fig. 6. Computational performance of the proposed model

VI. CONCLUSION

In this paper, a novel robust optimization model is proposed for HPPs offering regulating power in voluntary balancing

markets considering the uncertainty of regulating price, wind power, and activated regulating volumes. A nested adaptive column & constraint generation algorithm is developed to solve the proposed model. Based on the Danish test case, the main findings of this paper are:

1) Without considering the uncertainty of activated regulating volumes leads to aggressive offering and operation strategies for HPPs. Although utilizing the most conservative uncertainty set of wind power, the HPP in the studied case still fails to provide balancing services in around 6% of the time.

2) It is effective to model the uncertainty of activated regulating volumes using the decision dependent uncertainty set. The proposed model ensures the reliable provision of balancing services, avoiding being quarantined by transmission system operators.

3) The proposed algorithm is effective to solve the proposed model. In the studied case, the average solving time for the first run is 1408s, while it is 254s in the second run.

APPENDIX A

This appendix introduces how to select proper M values for the dual variables of the optimization problem (21d)-(21g). During each iteration l , after the SSP is solved and the optimal solution z_l^* is fixed, this optimization is written in the following compact formation:

$$\min_y c^T \cdot y \tag{25a}$$

$$s.t. Ay + b \leq 0 \tag{25b}$$

$$y \geq 0 \tag{25c}$$

Then, an auxiliary variable w and a penalization term $M \cdot w$ are added into the problem (25), resulting in the following optimization:

$$\min_y c^T \cdot y + M \cdot w \tag{26a}$$

$$s.t. Ay + b \leq w \tag{26b}$$

$$y, w \geq 0 \tag{26c}$$

Then, the M value can be gradually increased until the optimal solution $w^* = 0$, namely problem (25) and (26) are equivalent. According to dual theory, the dual problem of (26) is:

$$\max_{\lambda} b^T \cdot \lambda \tag{27a}$$

$$s.t. A \cdot \lambda \leq c \tag{27b}$$

$$0 \leq \lambda \leq M \tag{27c}$$

It is obvious that when $w^* = 0$, the M value is a natural bound of the dual variable λ .

ACKNOWLEDGMENT

This paper has received funding from the European Union's Horizon 2020 research and innovation programme under Marie Skłodowska-Curie grant agreement No. 861398. The authors would like to thank EUDP IEA Wind Task 50 - Hybrid Power Plants for the support of the work. The authors would like to thank Matti Koivisto, and Juan Pablo Murcia from Department of Wind and Energy Systems at Technical University of Denmark for their support for CorRES, and HPC cluster.

REFERENCES

- [1] W. Gorman, A. Mills, M. Bolinger, R. Wiser, N. G. Singhal, E. Ela, and E. O'Shaughnessy, "Motivations and options for deploying hybrid generator-plus-battery projects within the bulk power system," *The Electricity Journal*, vol. 33, no. 5, p. 106739, 2020.
- [2] S. Yu, F. Fang, Y. Liu, and J. Liu, "Uncertainties of virtual power plant: Problems and countermeasures," *Applied energy*, vol. 239, pp. 454–470, 2019.
- [3] Dykes Katherine, Jennifer King, Nicholas DiOrio, Ryan King, Vahan Gevorgian, Dave Corbus, Nate Blair, Kate Anderson, Greg Stark, Craig Turchi, Pat Moriarity, "Opportunities for research and development of hybrid power plants," *National Renewable Energy Laboratory (NREL)*, 2020.
- [4] WindEurope, "Renewable hybrid power plants: exploring the benefits and market opportunities," 2019, available <https://windeurope.org/policy/position-papers/renewable-hybrid-power-plants-exploring-the-benefits-and-market-opportunities/> Accessed in 2-23-2023.
- [5] Energinet, "Regulation c2: The balancing market and balance settlement," 2017.
- [6] —, "Regulation c3 handling of notifications and schedules," 2011.
- [7] Energinet, "Ancillary services to be delivered in Denmark - Tender conditions," <https://en.energinet.dk/media/cmpnizek/ancillary-services-to-be-delivered-in-denmark-tender-conditions-20-04-2023.pdf>, 2023, accessed: 06-05-2023.
- [8] K. Das, A. L. T. P. Grapperon, P. E. Sørensen, and A. D. Hansen, "Optimal battery operation for revenue maximization of wind-storage hybrid power plant," *Electric Power Systems Research*, vol. 189, p. 106631, 2020.
- [9] H. Ding, P. Pinson, Z. Hu, and Y. Song, "Optimal offering and operating strategies for wind-storage systems with linear decision rules," *IEEE Transactions on Power Systems*, vol. 31, no. 6, pp. 4755–4764, 2016.
- [10] I. L. Gomes, H. Pousinho, R. Melicio, and V. Mendes, "Stochastic coordination of joint wind and photovoltaic systems with energy storage in day-ahead market," *Energy*, vol. 124, pp. 310–320, 2017.
- [11] R. Zhu, K. Das, P. Sørensen, and A. Hansen, "Enhancing profitability of hybrid wind-battery plants in spot and balancing markets using data-driven two-level optimization," *Available at SSRN*, 2023.
- [12] X. Han and G. Hug, "A distributionally robust bidding strategy for a wind-storage aggregator," *Electric Power Systems Research*, vol. 189, p. 106745, 2020.
- [13] H. Khaloie, A. Anvari-Moghaddam, N. Hatzigaryriou, and J. Contreras, "Risk-constrained self-scheduling of a hybrid power plant considering interval-based intraday demand response exchange market prices," *Journal of Cleaner Production*, vol. 282, p. 125344, 2021.
- [14] H. Khaloie, M. Mollahassani-Pour, and A. Anvari-Moghaddam, "Optimal behavior of a hybrid power producer in day-ahead and intraday markets: a bi-objective cvar-based approach," *IEEE Transactions on Sustainable Energy*, vol. 12, no. 2, pp. 931–943, 2020.
- [15] H. Khaloie, A. Anvari-Moghaddam, J. Contreras, J.-F. Toubeau, P. Siano, and F. Vallée, "Offering and bidding for a wind producer paired with battery and caes units considering battery degradation," *International Journal of Electrical Power & Energy Systems*, vol. 136, p. 107685, 2022.
- [16] H. Khaloie, A. Anvari-Moghaddam, J. Contreras, and P. Siano, "Risk-involved optimal operating strategy of a hybrid power generation company: A mixed interval-cvar model," *Energy*, p. 120975, 2021.
- [17] J. L. Crespo-Vazquez, C. Carrillo, E. Diaz-Dorado, J. A. Martinez-Lorenzo, and M. Noor-E-Alam, "A machine learning based stochastic optimization framework for a wind and storage power plant participating in energy pool market," *Applied Energy*, vol. 232, pp. 341–357, 2018.
- [18] A. R. Silva, H. Pousinho, and A. Estanqueiro, "A multistage stochastic approach for the optimal bidding of variable renewable energy in the day-ahead, intraday and balancing markets," *Energy*, vol. 258, p. 124856, 2022.
- [19] S. Zhan, P. Hou, P. Enevoldsen, G. Yang, J. Zhu, J. Eichman, and M. Z. Jacobson, "Co-optimized trading of hybrid wind power plant with retired ev batteries in energy and reserve markets under uncertainties," *International Journal of Electrical Power & Energy Systems*, vol. 117, p. 105631, 2020.
- [20] E. Akbari, R.-A. Hooshmand, M. Gholipour, and M. Parastegari, "Stochastic programming-based optimal bidding of compressed air energy storage with wind and thermal generation units in energy and reserve markets," *Energy*, vol. 171, pp. 535–546, 2019.
- [21] J. L. Crespo-Vazquez, C. Carrillo, E. Diaz-Dorado, J. A. Martinez-Lorenzo, and M. Noor-E-Alam, "Evaluation of a data driven stochastic approach to optimize the participation of a wind and storage power plant in day-ahead and reserve markets," *Energy*, vol. 156, pp. 278–291, 2018.
- [22] R. A. Al-Lawati, J. L. Crespo-Vazquez, T. I. Faiz, X. Fang, and M. Noor-E-Alam, "Two-stage stochastic optimization frameworks to aid in decision-making under uncertainty for variable resource generators participating in a sequential energy market," *Applied Energy*, vol. 292, p. 116882, 2021.
- [23] Y. Wang, H. Zhao, and P. Li, "Optimal offering and operating strategies for wind-storage system participating in spot electricity markets with progressive stochastic-robust hybrid optimization model series," *Mathematical Problems in Engineering*, vol. 2019, 2019.
- [24] R. Zhu, K. Das, P. E. Sørensen, and A. D. Hansen, "Optimal participation of co-located wind-battery plants in sequential electricity markets," 2022.
- [25] O. Lindberg, D. Lingfors, J. Arqvist, D. van der Meer, and J. Munkhammar, "Day-ahead probabilistic forecasting at a co-located wind and solar power park in sweden: Trading and forecast verification," *Advances in Applied Energy*, p. 100120, 2023.
- [26] B. Xu, A. Oudalov, A. Ulbig, G. Andersson, and D. S. Kirschen, "Modeling of lithium-ion battery degradation for cell life assessment," *IEEE Transactions on Smart Grid*, vol. 9, no. 2, pp. 1131–1140, 2016.
- [27] eSett, "Nordic imbalance settlement handbook: Instructions and rules for market participants," 2023, available <https://www.esett.com/app/uploads/2023/06/NBS-Handbook-v4.4.pdf>. Accessed: 23-05-2023.
- [28] T. of Nordic countries, "Current requirements for production plans and imbalances, monitoring and the use of production plans in balancing," 2020, available https://nordicbalancingmodel.net/wp-content/uploads/2020/03/Current-requirements-for-production-plans-and-imbalances_FINAL.pdf. Accessed: 23-05-2023.
- [29] Y. Zhang, J. Wang, and X. Wang, "Review on probabilistic forecasting of wind power generation," *Renewable and Sustainable Energy Reviews*, vol. 32, pp. 255–270, 2014. [Online]. Available: <https://www.sciencedirect.com/science/article/pii/S1364032114000446>
- [30] T. Hong, P. Pinson, S. Fan, H. Zareipour, A. Troccoli, and R. J. Hyndman, "Probabilistic energy forecasting: Global energy forecasting competition 2014 and beyond," *International Journal of Forecasting*, vol. 32, no. 3, pp. 896–913, 2016. [Online]. Available: <https://www.sciencedirect.com/science/article/pii/S0169207016000133>
- [31] O. Lindberg, D. Lingfors, J. Arqvist, D. van der Meer, and J. Munkhammar, "Day-ahead probabilistic forecasting at a co-located wind and solar power park in sweden: Trading and forecast verification," *Advances in Applied Energy*, vol. 9, p. 100120, 2023. [Online]. Available: <https://www.sciencedirect.com/science/article/pii/S2666792422000385>
- [32] Norwegian Meteorological Institute, "Met norway thredds service," 2022. [Online]. Available: <https://thredds.met.no/>
- [33] R. Koenerker and G. Bassett, "Regression quantiles," *Econometrica*, vol. 46, no. 1, pp. 33–50, 1978. [Online]. Available: <http://www.jstor.org/stable/1913643>
- [34] M. Syakur, B. Khotimah, E. Rochman, and B. D. Satoto, "Integration k-means clustering method and elbow method for identification of the best customer profile cluster," in *IOP conference series: materials science and engineering*, vol. 336. IOP Publishing, 2018, p. 012017.
- [35] B. Zeng and L. Zhao, "Solving two-stage robust optimization problems using a column-and-constraint generation method," *Operations Research Letters*, vol. 41, no. 5, pp. 457–461, 2013.
- [36] Y. Chen and W. Wei, "Robust generation dispatch with strategic renewable power curtailment and decision-dependent uncertainty," *IEEE Transactions on Power Systems*, 2022.
- [37] L. Zhao and B. Zeng, "An exact algorithm for two-stage robust optimization with mixed integer recourse problems," *submitted, available on Optimization-Online.org*, 2012.
- [38] M. Koivisto, K. Das, F. Guo, P. Sørensen, E. Nuño, N. Cutululis, and P. Maule, "Using time series simulation tools for assessing the effects of variable renewable energy generation on power and energy systems," *Wiley Interdisciplinary Reviews: Energy and Environment*, vol. 8, no. 3, p. e329, 2019.
- [39] M. Koivisto, G. M. Jónsdóttir, P. Sørensen, K. Plakas, and N. Cutululis, "Combination of meteorological reanalysis data and stochastic simulation for modelling wind generation variability," *Renewable Energy*, vol. 159, pp. 991–999, 2020.
- [40] ENTSO-E, "ENTSO-E Transparency Platform," <https://transparency.entsoe.eu/dashboard/show>, accessed: 03-06-2021.
- [41] G. Van Rossum and F. L. Drake Jr, *Python tutorial*. Centrum voor Wiskunde en Informatica Amsterdam, The Netherlands, 1995.
- [42] IBM, "Docplex," <https://github.com/IBMDDecisionOptimization/docplex-doc>, Accessed: 12-01-2022.
- [43] Technical University of Denmark, "Sophia hpc cluster," *Research Computing at DTU*, 2019. [Online]. Available: <https://dtu-sophia.github.io/docs/>